Synthesis, Structure, and Hydrothiolation Activity of Rhodium Pyrazolylborate Complexes

Lauren R. Fraser, Jeffrey Bird, Qiming Wu, Changsheng Cao, Brian O. Patrick, and Jennifer A. Love*

Department of Chemistry, 2036 Main Mall, University of British Columbia, Vancouver, British Columbia V6T 1Z1, Canada

Received June 8, 2007

A series of rhodium pyrazolylborate complexes [$Tp^RRh(PPh_3)_2$] {Tp^R = HBR'_3, R′ = 3,5-dimethylpyrazolyl (**1**), pyrazolyl (**3**), 3-phenylpyrazolyl (**4**), or 3-phenyl-5-methylpyrazolyl (**5**)} and [Bp^R-$Rh(PPh_3)_2$] {$Bp^R = H_2BR'_2$, R′ = 3,5-dimethylpyrazolyl (2)} were prepared from [$ClRh(PPh_3)_3$] and KX (X = pyrazolylborate anion). Complexes **2**−**5** were characterized crystallographically. The solution structures of new complexes **4** and **5** were also examined by variable temperature NMR and IR spectroscopy. The catalytic activity of complexes **1**−**5** in alkyne hydrothiolation was then examined. It was found that disubstituted tris(pyrazolyl)borate complexes (**1** and **5**) give the best selectivity and yield in alkyne hydrothiolation with aliphatic thiols.

Introduction

Pyrazolylborates constitute an important class of multidentate, monoanionic ligands for transition metals.[1] Metal complexes bearing these ligands exhibit a broad range of catalytic and stoichiometric reactivity. Notably, rhodium pyrazolylborate complexes have been studied extensively for the stoichiometric activation of H−X bonds (X = H, C, S, etc.).[2] In comparison with pyrazolylborate complexes of other late transition metals,[3] the use of rhodium pyrazolylborate complexes in catalysis remains rare.[4] Nevertheless, a number of catalytic applications have emerged, including polymerization of phenylacetylene,[5] homogeneous hydrogenation of quinoline,[6] dimerization of terminal alkynes,[4] alkyne hydrophosphinylation,[7] aromatic C−H borylation,[8] hydrosilylation,[9] hydroarylation,[10] and hydroformylation.[11]

As part of our broader program focused on exploring the reactivity of transition metal-heteroatom bonds, we decided to investigate the catalytic activity of rhodium pyrazolylborate complexes for transformations of thiols. Transition metal-catalyzed reactions of thiols have been explored to a much lesser extent than those of amines, alcohols, and phosphines, due to the belief that sulfur compounds "poison" metal complexes, thereby precluding catalysis. Despite this generalization, a number of transition metal-catalyzed reactions involving thiols have been developed.[12] For instance, alkyne hydrothiolation (eq 1) is an attractive method for the formation of vinyl sulfides,

* Corresponding author. E-mail: jenlove@chem.ubc.ca.

(1) Trofimenko, S. In *Scorpionates-The Coordination Chemistry of Polypyrazolylborate Ligand*; Imperial College Press: London, 1999.

(2) For examples of stoichiometric bond activation reactions, see: C−H: (a) Ghosh, C. K.; Graham, W. A. G. *J. Am. Chem. Soc.* **1987**, *109*, 4726−4727. (b) Ghosh, C. K.; Hoyano, J. K.; Krentz, R.; Graham, W. A. G. *J. Am. Chem. Soc.* **1989**, *111*, 5480−5481. (c) Purwoko, A. A.; Lees, A. J. *Inorg. Chem.* **1995**, *34*, 424−425. (d) Paneque, M.; Taboada, S.; Carmona, E. *Organometallics* **1996**, *15*, 2678−2679. (e) Paneque, M.; Pérez, P. J.; Pizzano, A.; Poveda, M. L.; Taboada, S.; Trujillo, M.; Carmona, E. *Organometallics* **1999**, *18*, 4304−4310. (f) Wick, D. D.; Jones, W. D. *Organometallics* **1999**, *18*, 495−505. (g) Asplund, M. C.; Snee, P. T.; Yeston, J. S.; Wilkens, M. J.; Payne, C. K.; Yang, H.; Kotz, K. T.; Frei, H.; Bergman, R. G.; Harris, C. B. *J. Am. Chem. Soc.* **2002**, *124*, 10605−10612. (h) Rodriguez, P.; Díaz-Requejo, M. M.; Belderrain, T. R.; Trofimenko, S.; Nicasio, M. C.; Pérez, P. J. *Organometallics* **2004**, *23*, 2162−2167. Sn−H: (i) Cîrcu, V.; Fernandes, M. A.; Carlton, L. *Inorg. Chem.* **2002**, *41*, 3859−3865. S−H: (j) Cîrcu, V.; Fernandes, M. A.; Carlton, L. *Polyhedron* **2003**, *22*, 3293−3298.

(3) For examples of late transition metal pyrazolylborate complexes, see: with Cu: (a) Díaz-Requejo, M. M.; Nicasio, M. C.; Pérez, P. J. *Organometallics* **1998**, *17*, 3051−3057. (b) Díaz-Requejo, M. M.; Belderrain, T. R.; Nicasio, M. C.; Pérez, P. J. *Organometallics* **2000**, *19*, 285−289. (c) Díaz-Requejo, M. M.; Belderrain, T. R.; Pérez, P. J. *Chem. Commun.* **2000**, *19*, 1853−1854. (d) Morilla, M. E.; Molina, M. J.; Díaz-Requejo, M. M.; Belderrain, T. R.; Nicasio, M. C.; Trofimenko, S.; Pérez, P. J. *Organometallics* **2003**, *22*, 2914−2918. (e) Handy, S. T.; Ivanow, A.; Czopp, M. *Tetrahedron Lett.* **2006**, *47*, 1821−1823. with Ru: (f) Vicente, C.; Shul'pin, G. B.; Moreno, B.; Sabo-Etienne, S.; Chaudret, B. *J. Mol. Catal. A: Chem.* **1995**, *98*, L5−L8. (g) Chan, W.; Lau, C.; Chen, Y.; Fang, Y.; Ng, S.; Jia, G. *Organometallics* **1997**, *16*, 34−44. (h) Feng, Y.; Lail, M.; Barakat, K. A.; Cundari, T. R.; Gunnoe, T. B.; Petersen, J. L. *J. Am. Chem. Soc.* **2005**, *127*, 14174−14175. With Cu and Ru: (i) Singh, U. P.; Babbar, P.; Hassler, B.; Nishiyama, H.; Brunner, H. *J. Mol. Catal. A: Chem.* **2002**, *185*, 33−39. With Ni: (j) Kläui, W.; Turkowski, B.; Rheinwald, G.; Lang, H. *Eur. J. Inorg. Chem.* **2002**, *1*, 205−209. With Ni and Pd: (k) Santi, R.; Romano, A. M.; Sommazzi, A.; Grande, M.; Bianchini, C.; Mantovani, G. *J. Mol. Catal. A: Chem.* **2005**, *229*, 191−197.

(4) For catalytic transformations with TpRh complexes, see: Slugovc, C.; Padilla-Martinez, I.; Sirol, S.; Carmona, E. *Coord. Chem. Rev.* **2001**, *213*, 129−157.

(5) (a) Katayama, H.; Yamamura, K.; Miyaki, Y.; Ozawa, F. *Organometallics* **1997**, *16*, 4497−4500. (b) Ruman, T.; Ciunik, Z.; Trzeciak, A. M.; Wołowiec, S.; Ziołkowski, J. J. *Organometallics* **2003**, *22*, 1072−1080. (c) Trzeciak, A. M.; Ziołkowski, J. J. *Appl. Organomet. Chem.* **2004**, *18*, 124−129.

(6) Alvarado, Y.; Busolo, M.; Lopez-Linares, F. *J. Mol. Catal. A: Chem.* **1999**, *142*, 163−167.

(7) Van Rooy, S.; Cao, C.; Patrick, B. O.; Lam, A.; Love, J. A. *Inorg. Chim. Acta* **2006**, *359*, 2918−2923.

(8) Murata, M.; Odajima, H.; Watanabe, S.; Masuda, Y. *Bull. Chem. Soc. Jpn.* **2006**, *79*, 1980−1982.

(9) Ganicz, T.; Mizerska, U.; Moszner, M.; O'Brien, M.; Perry, R.; Stanczyk, W. A. *Appl. Catal. A: Gen.* **2004**, *259*, 49−55.

(10) Oxgaard, J.; Periana, R. A.; Goddard, W. A., III. *J. Am. Chem. Soc.* **2004**, *126*, 11658−11665.

(11) Trzeciak, A. M.; Borak, B.; Ciunik, Z.; Ziolkowski, J. J.; Guedes da Silva, M. F. C.; Pombeiro, A. J. L. *Eur. J. Inorg. Chem.* **2004**, *7*, 1411−1419.

(12) For examples of transition metal-catalyzed reactions involving thiols, see: (a) Kondo, T.; Mitsudo, T. *Chem. Rev.* **2000**, *100*, 3205−3220. (b) Togni, A., Grutzmacher, H., Eds. In *Catalytic Heterofunctionalization: From Hydroamination to Hydrozirconation*; Wiley-VCH: Weinheim, 2001; pp 289−251. (c) Alonso, F.; Beletskaya, I. P.; Yus, M. *Chem. Rev.* **2004**, *104*, 3079−3159.

10.1021/om700564t CCC: $37.00
Publication on Web 10/05/2007

which are valuable as synthetic intermediates in total synthesis[13] and as precursors to a wide range of functionalized molecules.[14] Although hydrothiolation with aryl thiols has been achieved in radical,[15] nucleophilic,[14s,16] and metal-catalyzed[17] reactions, alkyl thiols are typically unreactive.[17c] A selective method for the formation of *Z*-linear vinyl sulfides emerged in 2005,[14s] yet general methods for the stereo- and regiocontrolled synthesis of branched and *E*-linear alkyl vinyl sulfides remained elusive. We postulated that rhodium pyrazolylborate complexes would be sufficiently reactive to overcome this limitation.

Toward this goal, we recently disclosed that both Tp*Rh(PPh$_3$)$_2$ (**1**)[18,19] [Tp* = hydrotris(3,5-dimethylpyrazolyl)borate]

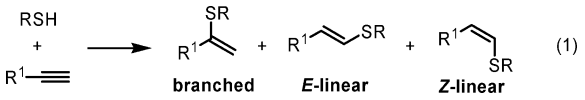

(1)

and Wilkinson's catalyst, ClRh(PPh$_3$)$_3$,[20] catalyze alkyne hydrothiolation with alkyl thiols. With both complexes, the reactions proceeded with good-to-excellent regioselectivities and yields. Reactions using ClRh(PPh$_3$)$_3$ provided the *E*-linear isomer preferentially, in agreement with Ogawa's results using aryl thiols.[17c] In comparison, reactions using Tp*Rh(PPh$_3$)$_2$ generated the branched isomer with high selectivity.[21] Intrigued by the reversal of regioselectivity depending on anionic ligand choice, we sought to evaluate a series of rhodium pyrazolylborate complexes for their activity in alkyne hydrothiolation. In particular, we were interested in exploring ligand denticity, as well as substitution of the pyrazolyl rings, as both the electron-donating ability and flexible modes of coordination (i.e., κ^2- versus κ^3-coordination) contribute to the unique properties of the tris(pyrazolyl)borate motif and thus can influence reactivity.

Tp^{R}RhLL′ complexes [Tp^R = substituted pyrazolylborate; L, L′ = ancillary ligands; Rh(I)] typically exist in an equilibrium of up to four isomers, **A**−**D** (Chart 1). Interconversion between

Chart 1. Isomers of Tris(pyrazolylborate) Rhodium Complexes

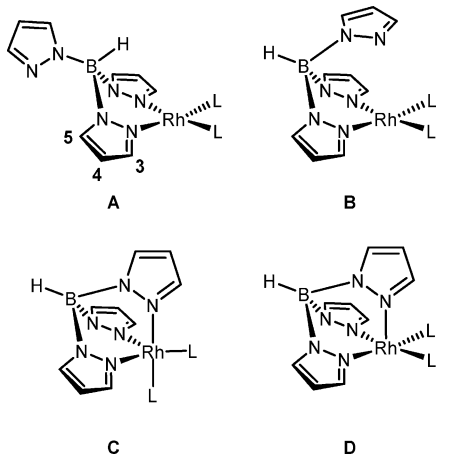

these species has been identified as crucial to the role of rhodium pyrazolylborates in stoichiometric C−H activation[2g,22] and is therefore expected to play a significant role in catalytic reactions involving bond activation. Isomers **A** and **B** are κ^2, 16-electron, square planar species; isomer **C** is a κ^3, 18-electron, trigonal bipyramidal species; and isomer **D** is a κ^3, 18-electron, square pyramidal species. Complexes with κ^3-coordination typically adopt trigonal bipyramidal geometry instead of square pyramidal geometry, as the latter would have a pyrazolyl ring bound in the apical position by an elongated Rh−N bond, which is considered unfavorable.[23] The equilibrium is dictated by the substitution pattern of the pyrazolyl rings (see isomer **A** in Chart

(13) For examples of vinyl sulfides as intermediates in total synthesis, see: (a) Bratz, M.; Bullock, W. H.; Overman, L. E.; Takemoto, T. *J. Am. Chem. Soc.* **1995**, *117*, 5958−5966. (b) Mizuno, H.; Domon, K.; Masuya, K.; Tanino, K.; Kuwajima, I. *J. Org. Chem.* **1999**, *64*, 2648−2656. (c) Pearson, W. H.; Lee, I. Y.; Mi, Y.; Stoy, P. *J. Org. Chem.* **2004**, *69*, 9109−9122.

(14) For examples of vinyl sulfides as precursors to functionalized or bioactive molecules, see: (a) Parham, W. E.; Blake, F. D.; Theissen, D. R. *J. Org. Chem.* **1962**, *27*, 2415−2419. (b) Trost, B. M.; Tanigawa, Y. *J. Am. Chem. Soc.* **1979**, *101*, 4743−4745. (c) Trost, B. M.; Ornstein, P. L. *J. Org. Chem.* **1982**, *47*, 748−751. (d) Metzner, P.; Thuillier, A. In *Sulfur Reagents in Organic Synthesis*; Academic Press: London, 1994. (e) Stiefel, E. I., Matsumoto, K., Eds. In *Transition Metal Sulfur Chemistry: Biological and Industrial Significance*; ACS Symposium Series 653; American Chemical Society: Washington, DC, 1996. (f) Roush, W. R.; Gwaltney, S. L.; Cheng, J.; Scheidt, K. A.; McKerrow, J. H.; Hansell, E. *J. Am. Chem. Soc.* **1998**, *120*, 10994−10995. (g) Adrio, J.; Carretero, J. C. *J. Am. Chem. Soc.* **1999**, *121*, 7411−7412. (h) Fernández, F.; Khiar, N. *Chem. Rev.* **2003**, *103*, 3651−3705. (i) Mauleon, P.; Nunez, A. A.; Alonso, I.; Carretero, J. C. *Chem.−Eur. J.* **2003**, *9*, 1511−1520. (j) Vedula, M. S.; Pulipaka, A. B.; Venna, C.; Chintakunta, V. K.; Jinnapally, S.; Kattuboina, V. A.; Vallakati, R. K.; Basetti, V.; Akella, V.; Rajgopal, S.; Reka, A. K.; Teepireddy, S. K.; Mamnoor, P. R.; Rajagopalan, R.; Bulusu, G.; Khandelwal, A.; Upreti, V. V.; Mamidi, S. R. *Eur. J. Med. Chem.* **2003**, *38*, 811−824. (k) Chen, M. S.; White, M. C. *J. Am. Chem. Soc.* **2004**, *126*, 1346−1347. (l) Farhat, S.; Zouev, I.; Marek, I. *Tetrahedron* **2004**, *60*, 1329−1337. (m) Sharma, V. M.; Seshu, K. V. A.; Sekhar, V. C.; Madan, S.; Vishnu, B.; Babu, P. A.; Krishna, C. V.; Sreenu, J.; Krishna, V. R.; Venkateswarlu, A.; Rajagopal, S.; Ajaykumarb, R.; Kumarb, T. S. *Bioorg. Med. Chem. Lett.* **2004**, *14*, 67−71. (n) Chumachenko, N.; Sampson, P.; Hunter, A. D.; Zeller, M. *Org. Lett.* **2005**, *7*, 3203−3206. (o) Dubbaka, S. R.; Vogel, P. *Angew. Chem., Int. Ed.* **2005**, *44*, 7674−7684. (p) Fernández, F.; Gómez, M.; Jansat, S.; Muller, G.; Martin, E.; Flores-Santos, L.; García, P. X.; Acosta, A.; Aghmiz, A.; Giménez-Pedró, M.; Masdeu-Bultó, A. M.; Diéguez, M.; Claver, C.; Maestro, M. A. *Organometallics* **2005**, *24*, 3946−3956. (q) Gumireddy, K.; Baker, S. J.; Cosenza, S. C.; Premila, J.; Kang, A. D.; Robell, K. A. *Proc. Nat. Acad. Sci.* **2005**, *102*, 1992−1997. (r) Gumireddy, K.; Reddy, V. R.; Cosenza, S. C.; Boominathan, R.; Baker, S. J.; Papathi, N. *Cancer Cell* **2005**, *7*, 275−286. (s) Kondoh, A.; Takami, K.; Yorimitsu, H.; Oshima, K. *J. Org. Chem.* **2005**, *70*, 6468−6473. (t) Marino, J. P.; Zou, N. *Org. Lett.* **2005**, *7*, 1915−1917. (u) Strebhardt, K.; Ullrich, A. *Nature Rev. Cancer* **2006**, *6*, 321−330.

(15) Radical reactions: (a) Patai, S., Ed. In *The Chemistry of the Thiol Group*; John Wiley & Sons, Ltd.: London, 1974; Vol. 2. (b) Ichinose, Y.; Wakamatsu, K.; Nozaki, K.; Birbaum, J. L.; Oshima, K.; Utimoto, K. *Chem. Lett.* **1987**, 1647−1650.

(16) Nucleophilic reactions: (a) Truce, W. E.; Simms, J. A. *J. Am. Chem. Soc.* **1956**, *78*, 2756−2759. (b) Truce, W.; Tichenor, G. J. W. *J. Organomet. Chem.* **1972**, *37*, 2391−2396.

(17) Metal-catalyzed reactions: using Pd: (a) Bäckvall, J. E.; Ericsson, A. *J. Org. Chem.* **1994**, *59*, 5850−5851. Using Pd, Rh, Ni, and Pt: (b) Kuniyasu, H.; Ogawa, A.; Sato, K. I.; Ryu, I.; Kambe, N.; Sonoda, N. *J. Am. Chem. Soc.* **1992**, *114*, 5902−5903. Using Pd, Rh, and Pt: (c) Ogawa, A.; Ikeda, T.; Kimura, K.; Hirao, T. *J. Am. Chem. Soc.* **1999**, *121*, 5108−5114. Using Rh and Ir: (d) Burling, S.; Field, L. D.; Messerle, B. A.; Vuong, K. Q.; Turner, P. *J. Chem. Soc., Dalton Trans.* **2003**, *21*, 4181−4191. Using Ru: (e) Koelle, U.; Rietmann, C.; Tjoe, J.; Wagner, T.; Englert, U. *Organometallics* **1995**, *14*, 703−713. Using Mo, Cr, and W: (f) McDonald, F. E.; Burova, S. A.; Huffman, L. G. *Synthesis* **2000**, *7*, 970−974. Using Ni: (g) Han, L. B.; Zhang, C.; Yazawa, H.; Shimada, S. *J. Am. Chem. Soc.* **2004**, *126*, 5080−5081. (h) Ananikov, V. P.; Malyshev, D. A.; Beletskaya, I. P.; Aleksandrov, G. G.; Eremenko, I. L. *Adv. Synth. Catal.* **2005**, *347*, 1993−2001. Using Pd and Ni: (i) Malyshev, D. A.; Scott, N. M.; Marion, N.; Stevens, E. D.; Ananikov, V. P.; Beletskaya, I. P.; Nolan, S. P. *Organometallics* **2006**, *25*, 4462−4470.

(18) Cao, C.; Fraser, L. R.; Love, J. A. *J. Am. Chem. Soc.* **2005**, *127*, 17614−17615.

(19) For a later use of Tp*RhL$_2$ complexes in alkyne hydrothiolation, see: Misumi, Y.; Seino, H.; Yasushi, M. *J. Organomet. Chem.* **2006**, *691*, 3157−3164.

(20) Shoai, S.; Bichler, P.; Kang, B.; Buckley, H.; Love, J. A. In preparation.

(21) For the first example of Pd-catalyzed hydrothiolation using alkyl thiols, see: Ananikov, V. P.; Orlov, N. V.; Beletskaya, I. P.; Khrustalev, V. N.; Antipin, M. Y.; Timofeeva, T. V. *J. Am. Chem. Soc.* **2007**, *129*, 7252−7253.

(22) Wiley, J. S.; Oldham, W. J.; Heinekey, D. M. *Organometallics* **2000**, *19*, 1670−1676.

(23) Webster, C. E.; Hall, M. B. *Inorg. Chim. Acta* **2002**, *330*, 268−282.

Scheme 1

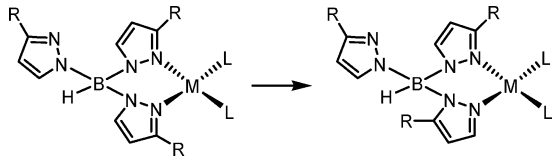

1 for numbering of the pyrazolyl ring) as well as the bulkiness of the ancillary ligands. κ^2-Coordination (i.e., forms **A** and **B**) predominates for tris(pyrazolyl)borate complexes with bulky substituents in the 3-position of the pyrazolyl rings and/or sterically bulky ancillary ligands. κ^3-Coordination (i.e., forms **C** and **D**) predominates for tris(pyrazolyl)borate complexes with smaller substituents on the pyrazolyl rings and/or less bulky ancillary ligands. In square planar complexes, the degree of substitution of the pyrazolyl rings dictates which form, **A** or **B**, is preferred. Complexes with substituents in the 3-position typically exist in form **A**, whereas unsubstituted pyrazolylborates or those with substitution in the 5-position typically exist in form **B**.[24]

In addition, depending on the position and extent of substitution of the pyrazolyl rings, rearrangement via a 1,2-borotropic shift can occur. This isomerization has been observed for a broad range of Tp^RM complexes (Scheme 1). The borotropic shift typically occurs for pyrazolylborates with 3- or 3,4-substitution[25a,c] to reduce van der Waals repulsion.[25b−d] Rearrangements in octahedral metal complexes with κ^3-bound tris(pyrazolyl)borate ligands have been well documented for complexes of a number of transition metals, including Co,[25a,26] Ti,[27] Mo,[25b] Ni,[26] and Fe.[26] In comparison, 1,2-borotropic shifts of square planar and tetrahedral tris(pyrazolyl)borate complexes are less common, although examples involving complexes of Rh,[25c,28] Ir,[25d] Zn,[28] Cd,[28] and Al[29] have been reported.

The interconversion of these isomers, along with additional fluxional processes, renders solution-phase assignment of Tp^R denticity challenging.[2j,23,24,25c,d,30] For example, the pyrazolyl rings can undergo rapid exchange on the NMR time scale, resulting in equivalence of these rings. Nevertheless, a combination of multinuclear[31] and variable temperature NMR spectroscopic experiments have allowed the solution-phase characterization of a number of Tp^RRhLL' complexes.[30e] In addition, IR stretching frequencies, particularly the ν(B−H) values, are diagnostic of κ^2 and κ^3 binding modes.[24,25c,d,30c,e] Generally, ν(B−H) < 2480 cm^{-1} indicates κ^2 binding and ν(B−H) > 2480 cm^{-1} indicates κ^3 binding.[30c]

Both solution and solid-state geometries of numerous Tp^RRhL_2 complexes where L is CO or olefin have been determined.[4b,23,24,25c,28,30a−c,f,h,i,32,33] In comparison, few examples of phosphine-containing rhodium tris(pyrazolyl)borate complexes have been structurally characterized.[11,30b,f−i,33,34] In 2001, Connelly and co-workers reported the structure of Tp*Rh(PPh$_3$)$_2$ in both solution and solid state;[30h] X-ray analysis shows that Tp*Rh(PPh$_3$)$_2$ adopts conformation **B** in the solid state. The IR spectrum showed a B−H stretching frequency of 2467 cm^{-1}, consistent with κ^2-coordination of the tris(pyrazolyl)borate ligand. Further evidence for κ^2 binding was obtained from ^{1}H and ^{31}P{^{1}H} NMR spectroscopy. At room temperature, two sets of signals were observed in the ^{1}H NMR spectrum for the pyrazolyl rings (2:1 ratio), indicating that two pyrazolyl rings are equivalent. In addition, the ^{31}P NMR spectrum revealed that both phosphines are equivalent, as a single resonance (δ 41.62, d, J_{Rh-P} = 175 Hz) was observed at room temperature. The coupling constant is typical of rhodium-phosphorus coupling. The two bound pyrazolyl rings, as well as the phosphines, are equivalent due to free rotation around the B−N bond of the free pyrazolyl ring. At −80 °C, three signals were observed for the pyrazolyl rings. Likewise, the ^{31}P NMR spectrum at −80 °C shows two doublets of doublets: δ 42.30, J_{Rh-P} = 179 Hz, $J_{P-P'}$ = 49 Hz and δ 39.18, $J_{Rh-P'}$ = 173 Hz, $J_{P-P'}$ = 51 Hz, indicating that the phosphines were no longer equivalent on the NMR time scale. Connelly suggested that the rotation of the free pyrazolyl ring is restricted at low temperature, resulting in inequivalence of the bound pyrazolyl rings and phosphines.

Connelly and co-workers also examined the solution structure of TpRh(PPh$_3$)$_2$.[30h] No assignment could be made on the basis

(24) Ministro, E. D.; Renn, O.; Ruegger, H.; Venanzi, L. M.; Burckhardt, U.; Gramlich, V. *Inorg. Chim. Acta* **1995**, *240*, 631−639.

(25) For explanations on 1,2-borotropic shift, see: (a) Trofimenko, S.; Calabrese, J. C.; Domaille, P. J.; Thompson, J. S. *Inorg. Chem.* **1989**, *28*, 1091−1101. (b) Cano, M.; Heras, J. V.; Jones, C. J.; McCleverty, J. A.; Trofimenko, S. *Polyhedron* **1990**, *9*, 619−621. (c) Bucher, U. E.; Currao, A.; Nesper, R.; Ruegger, H.; Venanzi, L. M.; Younger, E. *Inorg. Chem.* **1995**, *34*, 66−74. (d) Albinati, A.; Bovens, M.; Ruegger, H.; Venanzi, L. M. *Inorg. Chem.* **1997**, *36*, 5991−5999.

(26) Calabrese, J. C.; Trofimenko, S. *Inorg. Chem.* **1992**, *31*, 4810−4814.

(27) Rearrangements in octahedral titanium pyrazolylborate complexes: (a) LeCloux, D. D.; Keyes, M. C.; Osawa, M.; Reynolds, V.; Tolman, W. B. *Inorg. Chem.* **1994**, *33*, 6361−6368. (b) Murtuza, S.; Casagrande, O. L.; Jordon, R. F. *Organometallics* **2002**, *21*, 1882−1890. (c) Biagini, P.; Calderazzo, F.; Marchetti, F.; Romano, A. M.; Spera, S. *J. Organomet. Chem.* **2006**, *691*, 4172−4180.

(28) Rheingold, A. L.; White, C. B.; Trofimenko, S. *Inorg. Chem.* **1993**, *32*, 3471−3477.

(29) Looney, A.; Parkin, G. *Polyhedron* **1990**, *9*, 265−276.

(30) For solution phase studies of Tp^R denticity, see: (a) Bucher, U. E.; Fässler, T. F.; Hunziker, M.; Nesper, R.; Rüegger, H.; Venanzi, L. M. *Gazz. Chim. Ital.* **1995**, *125*, 181−188. (b) Chauby, V.; Serra-Le Berre, C.; Kalck, P.; Daran, J. C.; Commenges, G. *Inorg. Chem.* **1996**, *35*, 6534−6355. (c) Akita, M.; Ohta, K.; Takahashi, Y.; Hikichi, S.; Moro-oka, Y. *Organometallics* **1997**, *16*, 4121−4128. (d) Oldham, W. J.; Heinekey, D. M. *Organometallics* **1997**, *16*, 467−474. (e) Northcutt, T. O.; Lachicotte, R. J.; Jones, W. D. *Organometallics* **1998**, *17*, 5148−5152. (f) Ohta, K.; Hashimoto, M.; Takahashi, Y.; Hikichi, S.; Akita, M.; Moro-oka, Y. *Organometallics* **1999**, *18*, 3234−3240. (g) Akita, M.; Hashimoto, M.; Hikichi, S.; Moro-oka, Y. *Organometallics* **2000**, *19*, 3744−3747. (h) Connelly, N. G.; Emslie, D. J. H.; Geiger, W. E.; Hayward, O. D.; Linehan, E. B.; Orpen, A. G.; Quayle, M. J.; Rieger, P. H. *J. Chem. Soc., Dalton Trans.* **2001**, 670−683. (i) Malbosc, F.; Chauby, V.; Serra-Le Berre, C.; Etienne, M.; Daran, J. C.; Kalck, P. *Eur. J. Inorg. Chem* **2001**, *10*, 2689−2697.

(31) ^{11}B NMR spectroscopy is a technique that has been used to determine the coordination geometry around the metal. It was found that κ^2 complexes show resonances between δ −5.90 and −6.99 versus κ^3 complexes with resonances between δ −8.44 and −9.76 (see ref 30e). These resonances appear to be independent of both solvent and charge on the metal for group 9 and 10 metals (see ref 30e). Thus, there appears to be a strong correlation between the boron chemical shift and the denticity of the tris(pyrazolyl)borate ligand.

(32) Rhodium pyrazolylborate complexes with only CO or olefin as ancillary ligands: (a) Cocivera, M.; Ferguson, G.; Laior, F. J.; Szczecinski, P. *Organometallics* **1982**, *1*, 1139−1142. (b) Rheingold, A. L.; Ostrander, R. L.; Haggerty, B. S.; Trofimenko, S. *Inorg. Chem.* **1994**, *33*, 3666−3676. (c) Keyes, M. C.; Young, V. G.; Tolman, W. B. *Organometallics* **1996**, *15*, 4133−4140. (d) Sanz, D.; Maria, S.; Claramunt, R. M.; Cano, M.; Heras, J. V.; Campo, J. A.; Ruiz, F. A.; Pinilla, E.; Monge, A. *J. Organomet. Chem.* **1996**, *526*, 341−350.

(33) Rhodium pyrazolylborate monophosphine complexes: (a) Malbosc, F.; Kalck, P.; Daran, J. C.; Etienne, M. *J. Chem. Soc. Dalton Trans.* **1999**, 271−272. (b) Herberhold, M.; Eibl, S.; Milius, W.; Wrackmeyer, B. *Z. Anorg. Allg. Chem.* **2000**, *626*, 552−555.

(34) Rhodium pyrazolylborate bisphosphine complexes: (a) Baena, M. J.; Reyes, M. L.; Rey, L.; Carmona, E.; Nicasio, M. C.; Pérez, P. J.; Gutierrez, E.; Monge, A. *Inorg. Chim. Acta* **1998**, *273*, 244−254. (b) Hill, A. F.; White, A. J. P.; Williams, D. J.; Wilton-Ely, J. D. E. T. *Organometallics* **1998**, *17*, 3152−3154. (c) Paneque, M.; Sirol, S.; Trujillo, M.; Gutierrez-Puebla, E.; Monge, A.; Carmona, E. *Angew. Chem., Int. Ed.* **2000**, *39*, 218−221. (d) Paneque, M.; Sirol, S.; Trujillo, M.; Carmona, E.; Gutierrez-Puebla, E.; Monge, A.; Ruiz, C.; Malbosc, F.; Serra-Le Berre, C.; Kalck, P.; Etienne, M.; Daran, J. C. *Chem.−Eur. J.* **2001**, *7*, 3869−3879.

Chart 2. Rhodium Pyrazolylborate Complexes

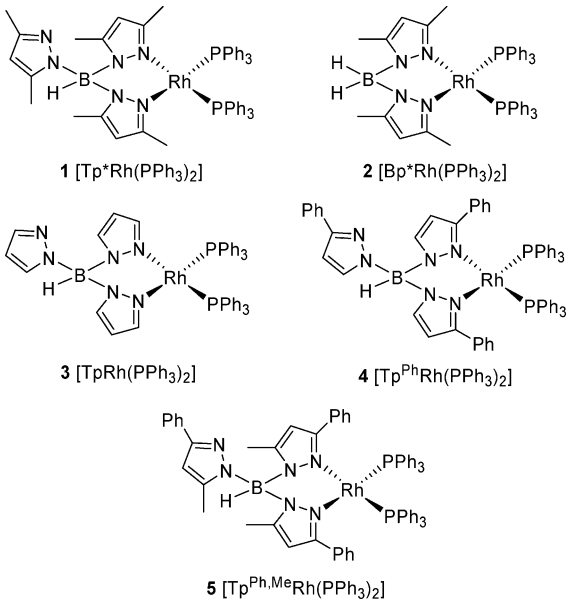

of the ^{1}H NMR spectrum, because of poor resolution even at low temperature. The ^{31}P NMR spectrum at room temperature showed a broad doublet, indicating equivalency of the phosphines. Unlike with Tp*Rh(PPh$_3$)$_2$, the phosphines did not become inequivalent at low temperature. Instead, at −80 °C, two doublets were observed, in approximately equal amounts. These were attributed to the presence of two isomers, in forms **A** and **B**. Further evidence for this assignment was obtained from the room-temperature IR spectrum, in which two B−H stretches were observed [ν(B−H) = 2414 cm^{-1} and 2394 cm^{-1}] in the typical range for κ^2 binding. The solid-state structure was not reported.

Given the significant influence of substituents on the geometry of tris(pyrazolyl)borate-metal complexes, we sought to determine the solution and solid-state structures of a series of rhodium complexes and to evaluate the influence of ligand structure on catalytic activity in the hydrothiolation of alkynes. The complexes selected for study are shown in Chart 2 {[HB(3,5-Me$_2$-pz)$_3$]$^-$ = Tp^{Me2} = Tp*; [H$_2$B(3,5-Me$_2$pz)$_2$]$^-$ = Bp^{Me2} = Bp*; [HB(pz)$_3$]$^-$ = Tp; [HB(3-Phpz)$_3$]$^-$ = Tp^{Ph}; [HB(3-Ph-5-Mepz)$_3$]$^-$ = Tp^{Ph,Me}}.

Results and Discussion

Synthesis and Structure of Rhodium Pyrazolylborate Complexes. Commercially available potassium tris(pyrazolyl)-borate salts were used to prepare complexes **1**, **3**, **4**, and **5**. The potassium bis(pyrazolyl)borate salt used for the synthesis of complex **2** was prepared by literature methods.[35] Known complexes **1**,[30h] **2**,[34a] and **3**[34b] and new complexes **4** and **5** were prepared by treating a solution of Wilkinson's catalyst in THF (toluene for complex **5**) with the appropriate potassium pyrazolylborate salt (KX, X = pyrazolylborate anion), at room temperature (Table 1). Upon workup, the corresponding rhodium pyrazolylborate complexes were obtained in good-to-excellent yields.

Of the known complexes (**1**,[2j,30h] **2**,[34a] and **3**[34b]), only complex **1** has been characterized crystallographically.[2j,30h] We were able to obtain crystals of **2**−**5** suitable for X-ray analysis by layering a saturated toluene solution of each complex with hexanes and cooling at −35 °C for approximately one week. The molecular structures are shown in Figures 1−4, and selected bond lengths and angles are presented in Table 2. All five solid-state structures clearly show κ^2-coordination of the Bp^R or Tp^R ligands, in agreement with the spectral data reported for complexes **1**[30h] and **3**[34b] and the solid-state structure of complex **1**.[30h] Complexes **2**−**5** all have approximately square planar geometry, with the sum of the angles about the rhodium atom ranging from 359.65 to 363.08°. In each complex, the rhodium atom is bound to two pyrazolyl rings, which form a six-membered ring chelate in a boat conformation, as well as two triphenylphosphine ligands. The bond angles and distances for **2**−**5** are comparable to those reported for complex **1**.[30h]

As mentioned earlier, complexes bearing tris(pyrazolyl)borate ligands with substituents in the 5-position of the pyrazolyl rings

(35) Trofimenko, S. *Inorg. Synth.* **1970**, *12*, 99−109.

Table 1. Synthesis of Rhodium Pyrazolylborate Complexes 1−5

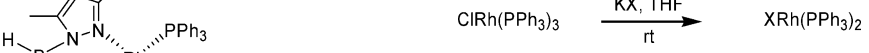

entry	X	complex	time (h)	yield (%)[a]	literature
1	Tp*	Tp*Rh(PPh$_3$)$_2$ (**1**)	1	92	48%,[b] 66%[c]
2	Bp*	Bp*Rh(PPh$_3$)$_2$ (**2**)	24	87	80%[d]
3	Tp	TpRh(PPh$_3$)$_2$ (**3**)	24	86	66%[e]
4	Tp^{Ph}	Tp^{Ph}Rh(PPh$_3$)$_2$ (**4**)	24	83	–
5	Tp^{Ph,Me}	Tp^{Ph,Me}Rh(PPh$_3$)$_2$ (**5**)	24	58[f]	–

[a] Isolated yields. [b] See ref 30h. [c] See ref 2j. [d] See ref 34a. [e] See ref 34b. [f] Toluene used as solvent in place of THF.

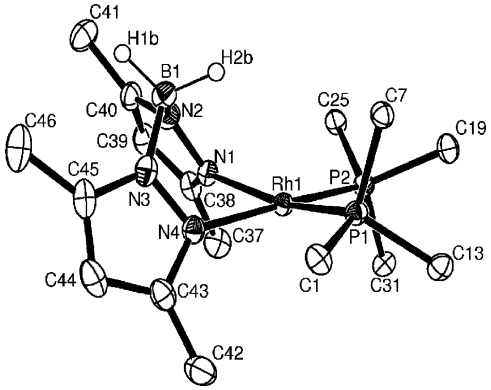

Figure 1. ORTEP diagram of complex **2**. Thermal ellipsoids are drawn at the 50% probability level. Hydrogen atoms, except for the B−H hydrogens, and phenyl groups of PPh$_3$ are excluded for clarity. Selected bond lengths (Å) and angles (deg) are given in Table 2 and crystallographic data is given in Table 3.

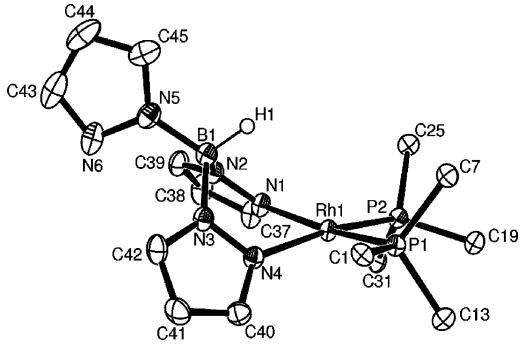

Figure 2. ORTEP diagram of complex **3**. Thermal ellipsoids are drawn at the 50% probability level. Hydrogen atoms, except for the B−H hydrogen, and phenyl groups of PPh$_3$ are excluded for clarity. Selected bond lengths (Å) and angles (deg) are given in Table 2 and crystallographic data is given in Table 3.

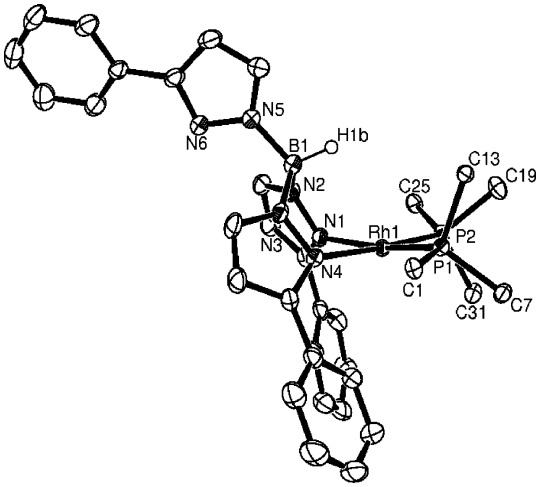

Figure 3. ORTEP diagram of complex **4**. Thermal ellipsoids are drawn at the 50% probability level. Hydrogen atoms, except for the B−H hydrogen, and phenyl groups of PPh_3 are excluded for clarity. Selected bond lengths (Å) and angles (deg) are given in Table 2 and crystallographic data is given in Table 3.

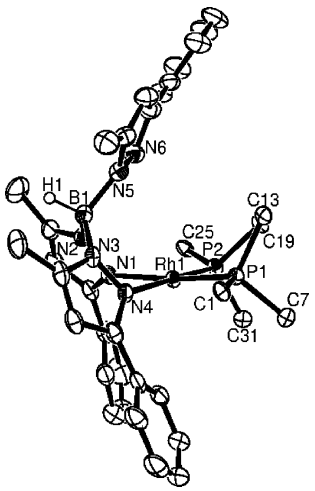

Figure 4. ORTEP diagram of complex **5**. Thermal ellipsoids are drawn at the 50% probability level. Hydrogen atoms, except for the B−H hydrogen, and phenyl groups of PPh_3 are excluded for clarity. Selected bond lengths (Å) and angles (deg) are given in Table 2 and crystallographic data is given in Table 3.

Table 2. Selected Bond Lengths (Å) and Angles (deg) for $Bp^*Rh(PPh_3)_2$ (2), $TpRh(PPh_3)_2$ (3), $Tp^{Ph}Rh(PPh_3)_2$ (4), and $Tp^{Ph,Me}Rh(PPh_3)_2$ (5)

	2	3	4	5
Rh−N(1)	2.132(2)	2.1575(1)	2.1240(2)	2.100(2)
Rh−N(4)	2.092(2)	2.1111(1)	2.1000(2)	2.140(2)
Rh−P(1)	2.2202(7)	2.2299(4)	2.2429(6)	2.2683(7)
Rh−P(2)	2.2468(7)	2.2558(4)	2.2618(6)	2.2572(7)
N(1)−Rh−N(4)	79.84(8)	83.37(5)	78.99(7)	77.49(8)
P(1)−Rh−P(2)	95.43(3)	93.60(2)	96.31(2)	94.15(3)
N(1)−Rh−P(1)	164.16(6)	169.58(4)	167.28(5)	173.25(6)
N(1)−Rh−P(2)	92.91(6)	92.98(4)	92.53(5)	92.42(6)
N(4)−Rh−P(1)	92.93(6)	91.52(3)	91.82(5)	96.18(6)
N(4)−Rh−P(2)	170.88(6)	169.18(4)	171.38(5)	167.66(6)

typically favor form **B**. The X-ray structures for complexes **1**[30h] and **3**−**5** are consistent with this trend. Complexes **1** and **5** exist in form **B** with the uncoordinated pyrazolyl ring pseudo parallel to the rhodium square plane. Complexes **3** and **4**, which lack substituents at the 5-position, are in form **A** with the uncoordinated pyrazolyl ring perpendicular to the rhodium square plane.

Complexes **1**−**5** were also characterized by variable temperature ^1H and $^{31}P\{^1H\}$ NMR spectroscopy, as well as IR spectroscopy. The spectroscopic data of complexes **2**[34a] and **3**[34b] are consistent with literature reports.[36] At room temperature, our spectral data for complex **1** matches that reported by Connelly. At low temperature, however, Connelly reported two doublets of doublets in the ^{31}P NMR spectrum and three distinct pyrazole resonances in the ^1H NMR spectrum at −80 °C.[30h] This data indicates that the pyrazole rings and phosphines are inequivalent at this temperature, presumably due to hindered rotation of the unbound pyrazole group. In comparison, we observe two broad doublets (δ 44.17, d, $J_{Rh-P} = 186$) and (δ 41.22, d, $J_{Rh-P} = 185$) in the $^{31}P\{^1H\}$ NMR spectrum and a 2:1 ratio of pyrazole signals in the ^1H NMR spectrum at −85 °C (Table 4). Presumably, in our study, rotation of the unbound pyrazolyl ring is slow but sufficiently rapid to render the two bound pyrazole rings equivalent on the ^1H NMR time scale.

The spectroscopic data of new complexes **4** and **5** are presented in Table 4. The NMR spectra of complex **4** obtained at both room temperature and −85 °C indicate κ^2-coordination of the pyrazolylborate ligand, consistent with the X-ray structure. The ^1H NMR spectra at both room temperature and −85 °C exhibits two pyrazole signals in a 2:1 ratio, and the $^{31}P\{^1H\}$ NMR spectrum shows a doublet at both room temperature (δ 46.89, d, $J_{Rh-P} = 178$ Hz) and at −85 °C (δ 46.69, d, $J_{Rh-P} = 176$ Hz). This data is consistent with free rotation of the free pyrazolyl ring, even at low temperature. From the spectroscopic and X-ray data for complex **4** there is no sign of a 1,2-borotopic shift, which has been observed with pyrazolylborate complexes with substitution only at the 3-position of the pyrazolyl rings.

The ^1H NMR spectrum of complex **5** at room temperature shows a 2:1 ratio of pyrazole signals, which is indicative of κ^2-coordination, in agreement with the X-ray data. At −85 °C, all of the pyrazolyl rings are inequivalent, suggesting restricted rotation about the B−N bond of the unbound pyrazolyl ring. The $^{31}P\{^1H\}$ NMR spectrum at room temperature is more complicated. The spectrum shows a doublet at δ 48.12 ($J_{Rh-P} = 182$ Hz) and a multiplet at δ 43.44−39.33, in a 1:5 ratio.[37] The VT-$^{31}P\{^1H\}$ NMR spectra are shown in Figure 5, and the chemical shifts are summarized in Table 5. As the temperature is decreased to −85 °C, the doublet (δ 48.12 $J_{Rh-P} = 182$ Hz) disappears and the multiplet resolves into two doublets of doublets (δ 42.60 $J_{Rh-P} = 178$, $J_{P-P'} = 50$ Hz; δ 39.42 $J_{Rh-P'} = 172$ Hz, $J_{P-P'} = 51$ Hz). This data could indicate that two species are present at room temperature, whereas one predominates at lower temperature. Alternatively, both species could be present at low temperature, if the peaks corresponding to the minor isomer are becoming broadened due to restricted rotation. The latter explanation seems more likely, as we do not observe coalescence of the two sets of peaks at lower temperatures. As the temperature is raised, the doublet observed at room-temperature remains unchanged, whereas the multiplet coalesces into a doublet.[38] The data for the major isomer is consistent with free rotation of the unbound pyrazolyl ring at elevated temperatures and restricted rotation just under room temperature. The two species could be forms **A** and **B**, or one could be the result of a 1,2-borotropic shift.

(36) For complex **3** our data is consistent with that reported by Connelly and coworkers (see ref 30h) but differs from the previously reported assigned spectra by Hill and coworkers (see ref 34b).

(37) The room temperature $^{31}P\{^1H\}$ NMR spectrum in d_8-toluene is more convoluted than in CD_2Cl_2.

(38) At elevated temperatures (100 °C) complex **5** decomposes, presumably to a rhodium hydrido species, as evidenced by the appearance of a hydride peak in the ^1H NMR.

Table 3. Crystallographic Data for Bp*Rh(PPh$_3$)$_2$ (2), TpRh(PPh$_3$)$_2$ (3), Tp^{Ph}Rh(PPh$_3$)$_2$ (4), and Tp^{Ph,Me}Rh(PPh$_3$)$_2$ (5)

	2	3	4	5
empirical formula	$C_{46}H_{46}BN_4P_2Rh.$ $^1/_2C_6H_{14}.^1/_2C_7H_8$	$C_{45}H_{40}BN_6P_2Rh.$ C_7H_8	$C_{63}H_{52}BN_6P_2Rh.$ C_5H_{12}	$C_{66}H_{58}BN_6P_2Rh.$ C_6H_{14}
formula weight	919.68	932.62	1140.91	1197.02
crystal color, habit	orange, prism	red, irregular	orange, irregular	red, irregular
crystal system	monoclinic	triclinic	monoclinic	monoclinic
space group	$P2_1/c$ (No. 14)	$P\bar{1}$ (No. 2)	$P2_1/n$ (No. 14)	$P2_1/n$ (No. 14)
crystal dimensions (mm^3)	0.25 × 0.25 × 0.40	0.20 × 0.20 × 0.10	0.035 × 0.10 × 0.20	0.05 × 0.12 × 0.25
a (Å)	a = 11.168(1)	12.2490(9)	17.4909(9)	14.9000(5)
b (Å)	b = 17.004(2)	13.637(1)	18.524(1)	14.8303(5)
c (Å)	c = 24.853(2)	14.971(1)	18.517(1)	29.460(1)
α (deg)	α = 90.0	112.004(3)	90.0	90.0
β (deg)	β = 98.470(6)	98.051(3)	107.914(5)	92.260(2)
γ (deg)	γ = 90.0	90.387(3)	90.0	90.0
Volume (Å^3)	4667.9(8)	2291.0(3)	5708.7(5)	6504.8(4)
Z	4	2	4	4
F(000)	1920.00	964.00	2376.00	2504.00
D_{calcd} (g/cm^3)	1.309	1.352	1.327	1.222
μ(Mo Kα) (cm^{-1})	4.74	4.86	4.03	3.57
λ(Mo Kα) (Å)	0.71073	0.71073	0.71073	0.71073
temp (K)	173	173	173	173
θ range (deg)	1.46−28.22	1.48−27.89	1.64−27.98	1.56−25.05
$2\theta_{max}$ (deg)	56.4	55.8	56.0	50.1
reflections collected	50326	77370	60965	49830
Independent reflections (R_{int})	11268 (0.052)	10812 (0.042)	13758 (0.044)	11499 (0.052)
max, min transmission	0.888, 0.802	0.953, 0.858	0.986, 0.839	0.982, 0.842
no. of variables	573	603	701	692
goodness of fit on F^2	1.02	1.11	1.02	0.99
final R_1 indices [on F, $I > 2\sigma(I)$]	0.039 (8528 reflections)	0.027 (9032 reflections)	0.037 (10811 reflections)	0.037 (8482 reflections)
wR2 indices (on F_2, all data)	0.098	0.064	0.094	0.090

Table 4. ^{1}H, ^{31}P{^{1}H} NMR and IR Spectroscopic Data for Rhodium Pyrazolylborate Complexes[a]

temp	^{1}H NMR	^{31}P-{^{1}H} NMR	IR/cm^{-1} ν(BH)[b]
	Tp*Rh(PPh$_3$)$_2$, 1		
25 °C	7.6−6.9 (m, 30H, P(C$_6$H$_5$)$_3$), 5.81 (s, 1H, pz H), 5.27 (s, 2H, pz H), 2.35 (s, 3H, CH$_3$), 2.27 (s, 6H, CH$_3$), 2.26 (s, 3H, CH$_3$), 1.79 (s, 6H, CH$_3$)	43.78 (d, J_{Rh-P} = 175 Hz)	2447
−85 °C	7.7−6.7 (m, 30H, P(C$_6$H$_5$)$_3$), 5.80 (s, 1H, pz H), 5.24 (br s, 2H, pz H), 4.35 (br s, 1H, BH), 2.51 (br s, 3H, CH$_3$), 2.28 (s, 6H, CH$_3$), 2.22 (br s, 6H, CH$_3$), 1.39 (br s, 3H, CH$_3$)	44.17 (br d, J_{Rh-P} = 186 Hz), 41.22 (br d, J_{Rh-P} = 185 Hz)	
	Tp^{Ph}Rh(PPh$_3$)$_2$, 4		
25 °C	8.26 (s, 1H, pz H), 7.97 (m, pz C$_6$H$_5$), 7.43 (s, 2H, pz H), 7.4−6.9 (m, 45H, PPh$_3$ + pz C$_6$H$_5$), 6.83 (s, 1H, pz H), 5.75 (s, 2H, pz H)	46.89 (d, J_{Rh-P} = 178 Hz)	2426
−85 °C	8.25 (s, 1H, pz H), 7.91 (m, pz C$_6$H$_5$), 7.37 (s, 2H, pz H), 7.4−6.9 (m, 45H, PPh$_3$ + pz C$_6$H$_5$), 6.81 (s, 1H, pz H), 5.73 (s, 2H, pz H)	46.69 (d, J_{Rh-P} = 176 Hz)	
	Tp^{Ph,Me}Rh(PPh$_3$)$_2$, 5		
25 °C	8.27 (d, J = 8.8 Hz, 4H, pz C$_6$H$_5$), 7.77 (d, J = 7.3 Hz, 2H, pz C$_6$H$_5$), 7.6−6.8 (m, 45H, PPh$_3$ + pz C$_6$H$_5$), 6.40 (s, 1H, pz H), 6.36 (s, 2H, pz H), 5.81 (s, 1H, BH), 2.51 (s, 6H, CH$_3$), 2.14 (s, 3H, CH$_3$)	MIN 48.12 (d, J_{Rh-P} = 182 Hz); MAJ 43.44−39.33 (m)	2463
−85 °C	8.24 (d, J = 7.3 Hz, 2H, pz C$_6$H$_5$), 7.76 (d, J = 7.3 Hz, 2H, pz C$_6$H$_5$), 7.6−6.8 (m, 45H, PPh$_3$ + pz C$_6$H$_5$), 6.38 (s, 1H, pz H), 6.03 (s, 1H, pz H), 5.74 (s, 1H, BH), 5.58 (s, 1H, pz H), 2.47 (s, 3H, CH$_3$), 2.46 (s, 3H, CH$_3$), 2.04 (s, 3H, CH$_3$)	MAJ 42.60 (dd, J_{Rh-P} = 178 Hz $J_{P-P'}$ = 50 Hz), 39.42 (dd, $J_{Rh-P'}$ = 172 Hz, $J_{P-P'}$ = 51 Hz)	

[a] Chemical shift (δ) in ppm. Spectra taken in CD_2Cl_2. [b] KBr pellet.

Structural assignments based on X-ray and spectroscopic analyses are summarized in Table 6. Complexes **1** and **3**−**5** all exist in the bidentate κ^2 form, which is supported by NMR and IR spectroscopy. Complexes **1** and **5** are present in form **B** in the solid state and complexes **3** and **4** are present in form **A**. This is consistent with literature reports that substituents in the 5-position of the pyrazolyl ring increases the predominance of form **B**.[24]

Comparison of Rhodium Pyrazolylborate Complexes in Catalytic Alkyne Hydrothiolation. With complexes **1**−**5** in hand, we were now ready to compare their reactivity and selectivity in catalytic hydrothiolation. A series of thiols and alkynes with varying degrees of functionality and steric bulk, were chosen for study (Chart 3).

Our exploration began using benzylthiol (**6**) and phenylacetylene (**10**) (Table 7). All reactions were carried out at room temperature, using 3 mol % of catalyst in a 1:1 mixture of 1,2-dichloroethane (DCE) and toluene. After 2 h, complex **1** gave a mixture of branched (**14a**) and *E*-linear (**14b**) products in 93% yield and 16:1 selectivity (Table 7, entry 1). In comparison, complexes **2**−**5** were all less efficient and provided lower selectivity. Higher yields were obtained with substituted tris-

Table 5. Variable Temperature ^{31}P NMR Spectroscopic Data for Complex 5

temperature	^{31}P{^{1}H} NMR chemical shifts
298 K	MIN δ 48.12 (d, J_{Rh-P} = 182 Hz); MAJ δ 43.44−39.33 (m)
273 K	MIN δ 48.15 (d, J_{Rh-P} = 180 Hz); MAJ δ 44.00−42.34 (m)
253 K	MIN δ 48.19 (d, J_{Rh-P} = 180 Hz); MAJ δ 43.14 (dd, J_{Rh-P} = 180, $J_{P-P'}$ = 51 Hz), δ 39.56 (dd, $J_{Rh-P'}$ = 174 Hz, $J_{P-P'}$ = 51 Hz)
233 K	MIN δ 48.23 (d, J_{Rh-P} = 180 Hz); MAJ δ 42.99 (dd, J_{Rh-P} = 180, $J_{P-P'}$ = 50 Hz), δ 39.51 (dd, $J_{Rh-P'}$ = 172 Hz, $J_{P-P'}$ = 50 Hz)
213 K	MIN δ 48.28 (d, J_{Rh-P} = 182 Hz); MAJ δ 43.83 (dd, J_{Rh-P} = 180, $J_{P-P'}$ = 50 Hz), δ 39.47 (dd, $J_{Rh-P'}$ = 174 Hz, $J_{P-P'}$ = 50 Hz)
188 K	MAJ δ 42.60 (dd, J_{Rh-P} = 180, $J_{P-P'}$ = 52 Hz), δ 39.42 (dd, $J_{Rh-P'}$ = 174 Hz, $J_{P-P'}$ = 52 Hz)

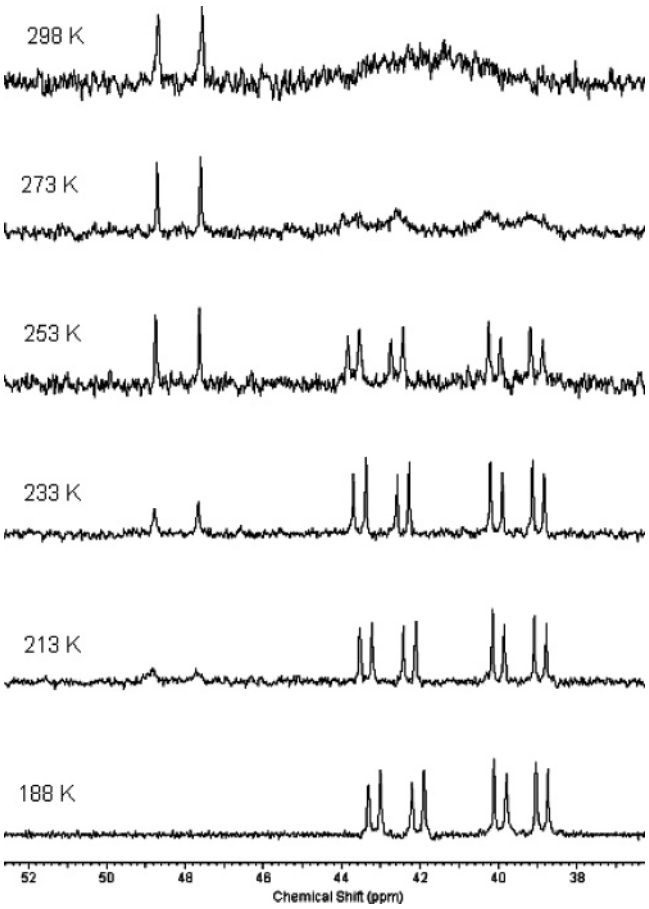

Figure 5. Variable temperature ^{31}P NMR spectra for complex **5** observed in CD_2Cl_2 at 162 MHz.

Table 6. Solid-State Structure Forms and/or Denticity of Complexes 1 and 3−5

complex	X-ray structure	NMR (denticity)	IR (denticity)
1	B (ref 2j, 30h)	κ^2 (ref 2j, 30h)	κ^2 (ref 30h)
3	A	κ^2 (ref 30h)	κ^2 (ref 30h)
4	A	κ^2	κ^2
5	B	κ^2	κ^2

(pyrazolyl)borate complexes **1**, **4**, and **5** than with complexes **2** or **3**. In fact, complex **3** was ineffective as a catalyst, producing the *Z*-linear product (**14c**) in low yield after extended reaction time. From this data, it appears that substitution at the 3-position and the ability of the ligand to achieve κ^3-coordination are important for catalytic activity.

The reaction of 2,2,2-trifluoroethanethiol (**7**) with phenylacetylene (**10**) using complexes **1**−**5** was used for further comparison (Table 8). Again, the highest yields were obtained for complexes **1**, **4**, and **5**. Likewise, better selectivity is obtained with tris(pyrazolyl)borate complexes than with the bis(pyrazolyl)borate complex, although the selectivity using 2,2,2-trifluoroethanethiol is lower than with benzylthiol.

Chart 3. Thiols and Alkynes

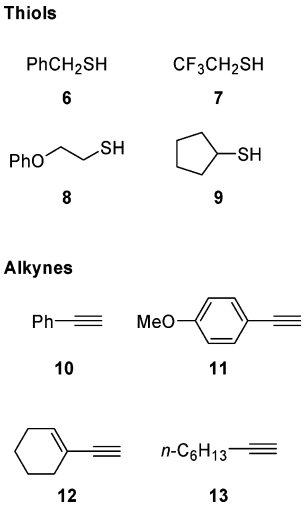

Table 7. Hydrothiolation of Phenylacetylene with Benzylthiol Catalyzed by Complexes 1−5

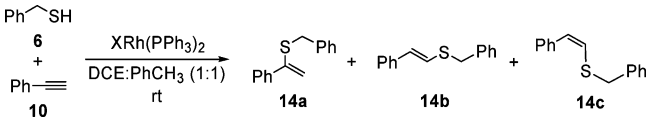

entry[a]	complex	time (h)	product ratio, yield[b]
1	Tp*Rh(PPh$_3$)$_2$	2	**14a:14b** (16:1), 93%[c]
2	Bp*Rh(PPh$_3$)$_2$	2	**14a:14b** (5:1), 55%
3	TpRh(PPh$_3$)$_2$	24	**14c**, 7%[d]
4	Tp^{Ph}Rh(PPh$_3$)$_2$	2	**14a:14b** (11:1), 87%[c]
5	Tp^{Ph,Me}Rh(PPh$_3$)$_2$	2	**14a:14b** (6:1), 78%[c]

[a] Reactions conducted with 3 mol% catalyst, 1.1 equiv thiol, 1.0 equiv alkyne. [b] Yields based on ^{1}H NMR spectroscopy using 1,3,5-trimethoxybenzene as an internal standard. [c] About 5−10% of an unidentified byproduct was observed. [d] Percent conversion with respect to benzylthiol.

The results presented in Tables 7 and 8 indicate that both ligand denticity and substitution of the pyrazolyl rings play a role in reaction efficiency and selectivity, as rhodium complexes bearing substituted tris(pyrazolyl)borate ligands are superior to those with either a bis(pyrazolyl)borate ligand or unsubstituted tris(pyrazolyl)borate ligand. We sought to further compare complexes **1**, **4**, and **5**, which contain substituted tris(pyrazolyl)borate ligands (Table 9). The reaction of 2-phenoxyethanethiol with phenylacetylene proceeded in high yield and selectivity with all three complexes, with the branched isomer being the exclusive product (entry 3). With a sterically hindered thiol, complex **5** provided the best yields (entries 4 and 5). With 1-ethynylcyclohexene (entry 5), all complexes showed complete selectivity for the alkyne over the alkene, as expected.[18] Complexes **1** and **5** performed comparably for the reaction of a terminal aliphatic alkyne with benzylthiol, whereas the yield

Table 8. Hydrothiolation of Phenylacetylene with 2,2,2-Trifluoroethanethiol Catalyzed by Complexes 1−5

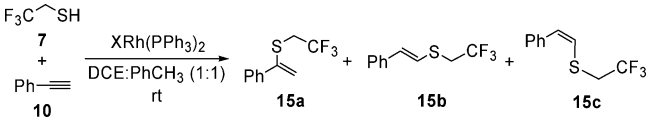

entry[a]	complex	time (h)	product ratio, yield[b]
1	$Tp^*Rh(PPh_3)_2$	2	**15a:15b** (3:1), 65%[c,d]
2	$Bp^*Rh(PPh_3)_2$	2	**15a:15b** (1:1), 32%[d]
3	$TpRh(PPh_3)_2$	48	**15b:15c** (1:3), 14%
4	$Tp^{Ph}Rh(PPh_3)_2$	2	**15a:15b** (4:1), 64%[c,d]
5	$Tp^{Ph,Me}Rh(PPh_3)_2$	2	**15a:15b** (3:1), 84%[c,d]

[a] Reactions conducted with 3 mol% catalyst, 1.1 equiv thiol, 1.0 equiv alkyne. [b] Yields based on ^{1}H NMR spectroscopy using 1,3,5-trimethoxybenzene as an internal standard. [c] About 5% of an unidentified byproduct was also observed. [d] Dimerization of phenylacetylene dimer also observed (∼5%).

Table 9. Substrate Scope of Alkyne Hydrothiolation Catalyzed by Complexes 1, 4, and 5

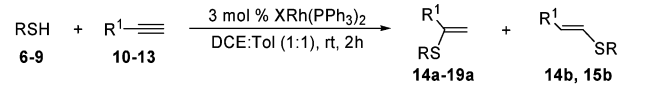

Entry	Thiol 1.1 equiv.	Alkyne 1.0 equiv.	Ratio, Yield[a] Complex **1**	Ratio, Yield[a] Complex **4**	Ratio, Yield[a] Complex **5**
1[b]	$PhCH_2SH$ **6**	Ph— **10**	**14a:14b** (16:1) 93%	**14a:14b** (11:1) 87%	**14a:14b** (6:1) 78%
2[b,c]	CF_3CH_2SH **7**	Ph— **10**	**15a:15b** (3:1) 65%	**15a:15b** (4:1) 64%	**15a:15b** (3:1) 84%
3	PhO SH MeO— **8** **11**		**16a** >95%	**16a** >95%	**16a** >95%
4[b]	SH MeO— **9** **11**		**17a** 61%	**17a** 73%	**17a** 75%
5[b,d]	SH **9**	**12**	**18a** 56%	**18a** 60%	**18a** 80%
6	$PhCH_2SH$ **6**	n-C_6H_{13}— **13**	**19a** >95%	**19a** 71%	**19a** >95%

[a] Yields based on ^{1}H NMR spectroscopy using 1,3,5-trimethoxybenzene as an internal standard. [b] An unidentified product was found in <10% yield for entries 1, 2, and 5 by ^{1}H NMR spectroscopy. [c] Contained <5% yield of the *E*-linear phenylacetylene dimer. [d] Yield after 3 h.

with complex **4** was considerably lower.[39] Overall, complexes **1** and **5** are superior to complex **4**, suggesting that substitution at both the 3- and 5-positions of the pyrazolyl ring are important for reactivity and selectivity. It is noteworthy that these two complexes that exist in form **B** in the solid state and are the best catalysts.

Conclusions

We have prepared a series of bis and tris(pyrazolyl)borate complexes to explore the structural features responsible for catalytic activity in alkyne hydrothiolation reactions using alkyl thiols. The rhodium complexes were characterized in the solid state and in solution, using variable temperature ^{1}H NMR and ^{31}P{^{1}H} NMR spectroscopy, as well as IR spectroscopy. All complexes show κ^2-coordination in the solid state. Complexes **1**[2j,30h] and **5**, which have substituents at the 5-position of the pyrazolyl rings, exist in form **B**, whereas complexes **3** and **4**, which lack substituents at the 5-position, exist in form **A**. The solution-phase spectroscopic data also indicates κ^2-coordination, as well as dynamic processes, presumably involving rotation about the B−N bond of the unbound pyrazolyl ring. In catalytic hydrothiolation, complexes with substituted tris(pyrazolyl)borate ligands gave better yields and selectivities than the substituted bis(pyrazolyl)borate complex, suggesting that the ability to adopt κ^3-coordination is crucial for catalysis. In addition, complexes with substituted pyrazolyl rings outperformed those without substitution. Furthermore, complexes with substitution in the 3- and 5-positions of the pyrazolyl ring were better than the complex with substitution at only the 3-position. Mechanistic investigations into catalytic hydrothiolation are currently underway and are expected to reveal further information about the role of denticity and pyrazolylborate substitution.

Experimental Section

General Procedures. Manipulation of inorganic compounds was performed using standard Schlenk techniques in a nitrogen-filled MBraun or Vacuum Atmospheres drybox (O_2 < 2 ppm). NMR spectra were recorded on Bruker Avance 300 MHz or Bruker Avance 400 MHz spectrometers. ^{1}H, ^{13}C{^{1}H}, and ^{31}P{^{1}H} NMR spectra are reported in parts per million and were referenced to residual solvent. Coupling constant values were extracted assuming first-order coupling. The multiplicities are abbreviated as follows: s = singlet, d = doublet, q = quartet, m = multiplet, br d = broad doublet, and dd = doublet of doublets. ^{31}P{^{1}H} NMR spectra were referenced to an external 85% H_3PO_4 standard. All spectra were obtained at 25 °C, unless otherwise stated. GC spectra were recorded on a Varian CP-3800 or an HP 5890 Series II gas chromatograph. Mass spectra were recorded on a Kratos MS-50 mass spectrometer. MALDI specta were recorded on a Bruker biflex IV mass spectrometer.

Materials and Methods. Pentane, hexanes, dichloromethane, 1,2-dichloroethane, THF, and toluene were dried by passage through solvent purification columns.[40] CD_2Cl_2 was purchased in 1 g ampules and used without further purification. Compounds **6**−**10** and **12** were obtained from commercial sources and were degassed by freeze−pump−thaw before being brought into the drybox. Compounds **11** and **13** were also obtained from commercial sources and were distilled over 4 Å molecular sieves and were degassed by freeze−pump−thaw before being brought into the drybox. Wilkinson's catalyst [$ClRh(PPh_3)_3$] was purchased from Strem Chemicals and was used without further purification. Spectroscopic data for known organics: **14a**,[18] **14b**,[41] **14c**,[12a] **15b**,[20] **16a**,[18] and **19a**[18] were consistent with literature values.

Synthesis of [Tp*Rh(PPh$_3$)$_2$] (1). In the glove box, $ClRh(PPh_3)_2$ (202 mg, 0.22 mmol) was weighed into a 20 mL vial equipped with a Teflon stir bar. KTp* (74 mg, 0.22 mmol) and THF (4 mL) were then added sequentially. The vial was covered with a plastic cap and the solution was stirred at room temperature. The solution changed color from maroon to orange within 10 min. After stirring for 1 h, the volatiles were removed under reduced pressure. The residue was dissolved in toluene (2 mL) and was layered with hexanes (8 mL). The solution was cooled to −35 °C; after 7 days, orange crystals formed. The solution was decanted, and the crystals

(39) Alkyl vinyl sulfide **19a** isomerizes to the internal olefin over prolonged exposure to the catalyst (see ref 18). However, at short reaction times, the 1,1-disubstituted alkene can be obtained selectively.

(40) Pangborn, A. B.; Giardello, M. A.; Grubbs, R. H.; Rosen, R. K.; Timmers, F. J. *Organometallics* **1996**, *15*, 1518−1520.

(41) Zheng, Y.; Du, X.; Bao, W. *Tetrahedron Lett.* **2006**, *47*, 1217−1220.

were washed with 4 × 5 mL of hexanes. The product was dried under reduced pressure to give 187 mg (92%) of an orange crystalline solid. Room temperature ^{1}H and ^{31}P{^{1}H} NMR data, as well as IR data, were consistent with literature reports.[2j,30h] Low-temperature NMR indicates equivalence of two pyrazoles, whereas Connelly reports the inequivalence of all three pyrazoles (see Results and Discussion section).

Synthesis of [Bp*Rh(PPh$_3$)$_2$] (2). In the glove box, ClRh(PPh$_3$)$_2$ (103 mg, 0.11 mmol) was weighed into a 20 mL vial equipped with a Teflon stir bar. KBp* (39 mg, 0.16 mmol) and THF (2 mL) were then added sequentially. The vial was covered with a plastic cap and the solution was stirred at room temperature. The solution changed color from maroon to orange within 10 min. After stirring for 24 h, the volatiles were removed under reduced pressure. The residue was dissolved in toluene (2 mL) and was layered with hexanes (8 mL). The solution was cooled to −35 °C; after 7 days orange crystals formed. The solution was decanted and the crystals were washed with 4 × 5 mL of hexanes. The product was dried under reduced pressure to give 80 mg (87%) of an orange crystalline solid. ^{1}H and ^{31}P{^{1}H} NMR data, as well as IR data, were consistent with literature values.[34a]

Synthesis of [TpRh(PPh$_3$)$_2$] (3). In the glove box, ClRh(PPh$_3$)$_2$ (200 mg, 0.22 mmol) was weighed into a 20 mL vial equipped with a Teflon stir bar. KTp (80 mg, 0.32 mmol) and THF (3 mL) were then added sequentially. The vial was covered with a plastic cap and the solution was stirred at room temperature. The solution changed color from maroon to orange within 10 min. After stirring for 24 h, the volatiles were removed under reduced pressure. The residue was dissolved in toluene (2 mL) and was layered with hexanes (8 mL). The solution was cooled to −35 °C; after 12 days orange crystals formed. The solution was decanted and the crystals were washed with 4 × 5 mL of hexanes. The product was dried under reduced pressure to give 155 mg (86%) of an orange crystalline solid. ^{1}H and ^{31}P{^{1}H} NMR data, as well as IR data, are tabulated in Table 4. ^{1}H and ^{31}P{^{1}H} NMR data, as well as IR data, were consistent with literature values.[34b]

Synthesis of [Tp^{Ph}Rh(PPh$_3$)$_2$] (4). In the glove box, ClRh(PPh$_3$)$_2$ (100 mg, 0.11 mmol) was weighed into a 20 mL vial equipped with a Teflon stir bar. KTp^{Ph} (84 mg, 0.17 mmol) and THF (2 mL) were then added sequentially. The vial was covered with a plastic cap and the solution was stirred at room temperature. The solution changed color from maroon to orange within 10 min. After stirring for 24 h, the volatiles were removed under reduced pressure. The residue was dissolved in toluene (2 mL) and was layered with hexanes (8 mL). The solution was cooled to −35 °C; after 7 days, orange crystals formed. The solution was decanted and the crystals were washed with 4 × 5 mL of hexanes. The product was dried under reduced pressure to give 96 mg (83%) of an orange crystalline solid. ^{1}H NMR (CD_2Cl_2, 400 MHz) at 25 °C: 8.26 (s, 1H, pz H), 7.97 (m, pz C_6H_5), 7.43 (s, 2H, pz H), 7.4−6.9 (m, 45H, PPh$_3$ + pz C_6H_5), 6.83 (s, 1H, pz H), 5.75 (s, 2H, pz H); at −85 °C: 8.25 (s, 1H, pz H), 7.91 (m, pz C_6H_5), 7.37 (s, 2H, pz H), 7.4−6.9 (m, 45H, PPh$_3$ + pz C_6H_5), 6.81 (s, 1H, pz H), 5.73 (s, 2H, pz H). ^{31}P{^{1}H} NMR (CD_2Cl_2, 162 MHz) at 25 °C: 46.89 (d, J_{Rh-P} = 178 Hz); at −85 °C: 46.69 (d, J_{Rh-P} = 176 Hz). IR (KBr Pellet) at 25 °C: 2426 [ν(B−H)] cm^{-1}. LRMS (EI) *m*/*z* calcd for $C_{63}H_{52}BN_6P_2Rh$: 1068.29; found: 262 (PPh$_3$, $C_{18}H_{15}P$), 806 [Tp^{Ph}Rh(PPh$_3$), $C_{45}H_{37}BN_6PRh$]. HRMS (EI) *m*/*z* calcd for Tp^{Ph}Rh(PPh$_3$), $C_{45}H_{37}BN_6PRh$: 806.1965; found: 806.1951. MALDI *m*/*z* calcd for $C_{63}H_{52}BN_6P_2Rh$: 1068; found: 1068.

Synthesis of [Tp^{Ph,Me}Rh(PPh$_3$)$_2$] (5). In the glove box, ClRh(PPh$_3$)$_2$ (101 mg, 0.11 mmol) was weighed into a 20 mL vial equipped with a Teflon stir bar. KTp^{Ph,Me} (87 mg, 0.17 mmol) and toluene (2 mL) were then added sequentially. The vial was covered with a plastic cap and the solution was stirred at room temperature. The solution changed color from maroon to orange within 10 min. After stirring for 24 h, the volatiles were removed under reduced pressure. The residue was dissolved in toluene (2 mL) and was layered with hexanes (8 mL). The solution was cooled to −35 °C; after 7 days orange crystals formed. The solution was decanted and the crystals were washed with 4 × 5 mL of hexanes. The product was dried under reduced pressure to give 70 mg (58%) of an orange crystalline solid. ^{1}H NMR (CD_2Cl_2, 400 MHz) at 25 °C: 8.27 (d, J = 8.8 Hz, 4H, pz C_6H_5), 7.77 (d, J = 7.3 Hz, 2H, pz C_6H_5), 7.6−6.8 (m, 45H, PPh$_3$ + pz C_6H_5), 6.40 (s, 1H, pz H), 6.36 (s, 2H, pz H), 5.81 (s, 1H, BH), 2.51 (s, 6H, CH_3), 2.14 (s, 3H, CH_3); at −85 °C: 8.24 (d, J = 7.3 Hz, 2H, pz C_6H_5), 7.76 (d, J = 7.3 Hz, 2H, pz C_6H_5), 7.6−6.8 (m, 45H, PPh$_3$ + pz C_6H_5), 6.38 (s, 1H, pz H), 6.03 (s, 1H, pz H), 5.74 (s, 1H, BH), 5.58 (s, 1H, pz H), 2.47 (s, 3H, CH_3), 2.46 (s, 3H, CH_3), 2.04 (s, 3H, CH_3). ^{31}P{^{1}H} NMR (CD_2Cl_2, 162 MHz) at 25 °C: 48.12 (d, J_{Rh-P} = 182 Hz), 43.44−39.33 (m); at −85 °C: 42.60 (dd, J_{Rh-P} = 178 Hz, J_{P-P} = 50 Hz), 39.42 (dd, J_{Rh-P} = 172 Hz, J_{P-P} = 51 Hz). IR (KBr Pellet) at 25 °C: 2463 [ν(B−H)] cm^{-1}. LRMS (EI) *m*/*z* calcd for $C_{66}H_{58}BN_6P_2Rh$: 1110.33; found: 262 (PPh$_3$, $C_{18}H_{15}P$), 848 [Tp^{Ph,Me}Rh(PPh$_3$), $C_{48}H_{43}BN_6PRh$]. HRMS (EI) *m*/*z* calcd for Tp^{Ph,Me}Rh(PPh$_3$), $C_{48}H_{43}BN_6PRh$: 848.2435; found: 848.2429. MALDI *m*/*z* calcd for $C_{66}H_{58}BN_6P_2Rh$: 1110; found: 848.6. Anal. Calcd for $C_{66}H_{58}BN_6P_2Rh$: C, C, 71.36; H, 5.26; N, 7.57; found: C, 71.52; H, 5.42; N, 7.37.

General Experimental Procedure for Catalytic Hydrothiolation. Tp*Rh(PPh$_3$)$_2$ (9 mg, 0.01 mmol, 3 mol %), 1,3,5-trimethoxybenzene (17 mg, 0.10 mmol, 0.33 equiv.), toluene (125 μL) and 1,2-dichloroethane (125 μL) were combined in the glove box in a 5 mL vial equipped with a magnetic stir bar and a screw cap. 2,2,2-Trifluoroethanethiol (30 μL, 0.34 mmol, 1.1 equiv) and phenylacetylene (34 μL, 0.31 mmol, 1.0 equiv) were added sequentially. The vial was capped and was removed from the glovebox. The vial was then wrapped in foil and the solution was stirred at room temperature for 2 h. The solution was concentrated under vacuum. The residue was dissolved in ~1 mL of $CDCl_3$ and the resulting solution was analyzed by ^{1}H NMR spectroscopy. The yield was determined to be 65%, based using 1,3,5-trimethoxybenzene as an internal standard. The solution was then transferred to a 20 mL vial and petroleum ether (boiling range 35−60 °C) was added to precipitate the rhodium complex. The solution was filtered through silica gel and the resulting solution was concentrated under vacuum. Flash chromatography (SiO_2, 10% ethyl acetate/petroleum ether as eluant) provided the product. Analytical data was consistent with spectroscopic data.

(2,2,2-Trifluoroethyl)(1-phenylvinyl)sulfane (15a): light-yellow oil; 10% ethyl acetate/petroleum ether used as eluant for flash chromatography. ^{1}H NMR ($CDCl_3$, 300 MHz): δ 7.52−7.34 (m, 5H), 5.58 (s, 1H), 5.52 (s, 1H), 3.08 (q, 2H, J = 9.7 Hz). ^{13}C{^{1}H} NMR ($CDCl_3$, 400 MHz): δ 134.0, 129.5, 129.2, 128.9, 128.8, 127.9, 117.6, 38.6. HRMS (EI) *m*/*z* calcd for $C_{10}H_9SF_3$: 218.0377; found: 218.0373.

(*Z*)-(2,2,2-Trifluoroethyl)(2-phenylvinyl)sulfane (15c): light-yellow oil. ^{1}H NMR ($CDCl_3$, 400 MHz): δ 7.46−7.29 (m, 5H), 6.53 (d, 1H, J = 10.7 Hz), 6.19 (d, 1H, J = 10.7 Hz), 3.33 (q, 2H, J = 10.7 Hz). ^{13}C{^{1}H} NMR ($CDCl_3$, 400 MHz): δ 136.4, 136.2, 132.1, 128.9, 128.6, 128.2, 127.6, 37.7. HRMS (EI) *m*/*z* calcd for $C_{10}H_9SF_3$: 218.0377; found: 218.0384.

Cyclopentyl(1-(4-methoxyphenyl)vinyl)sulfane (17a): orange oil; 10% ethyl acetate/petroleum ether used as eluant for flash chromatography. ^{1}H NMR ($CDCl_3$, 300 MHz): δ 7.59 (d, 2H, J = 9.0 Hz), 6.95 (d, 2H, J = 9.0 Hz), 5.50 (s, 1H), 5.26 (s, 1H), 3.87 (s, 3H), 3.43 (m, 1H), 2.10 (m, 2H), 1.68 (m, 6H). ^{13}C{^{1}H} NMR ($CDCl_3$, 300 MHz): δ 159.9, 145.4, 132.7, 129.2, 128.5, 125.5, 113.8, 110.6, 55.4, 44.2, 33.3, 25.2. HRMS (EI) *m*/*z* calcd for $C_{14}H_{18}OS$: 234.1078; found: 234.1074.

1-(Cyclohexylvinyl)(cyclopentyl)sulfane (18a): light-yellow oil; 5% ethyl acetate/petroleum ether used as eluant for flash chromatography. ^{1}H NMR ($CDCl_3$, 300 MHz): δ 6.25 (m, 1H), 5.29 (s,

1H), 4.99 (s, 1H), 3.35 (m, 1H), 2.23 (m, 2H), 2.16 (m, 2H), 2.00 (m, 2H), 1.63 (m, 10H). $^{13}C\{^1H\}$ NMR ($CDCl_3$, 300 MHz): δ 162.5, 128.1, 109.1, 93.9, 44.7, 34.1, 27.9, 26.7, 25.7, 23.9, 23.1. HRMS (EI) *m*/*z* calcd for $C_{13}H_{20}S$: 208.1286; found: 208.1279.

X-Ray Crystal Structures of 2−5. Crystal intensity collection, and refinement details are summarized in the Supporting Information as Tables S1, S7, S13, and S19. All measurements for complexes **2**, **4**, and **5** were made on a Bruker X8 APEX II diffractometer and all measurements for complex **3** were made on a Bruker X8 APEX diffractometer, both with graphite monochromated Mo−Kα radiation. Data were collected in a series of ϕ and ω scans and subsequently processed with the Bruker SAINT[42] software package. Data were corrected for absorption effects using the multiscan technique (SADABS).[43] The data were corrected for by Lorentz and polarization effects. The structures were solved using direct methods[44] and refined using SHELXTL.[45] For complexes **2**−**5** all non-hydrogen atoms were refined anisotropically, whereas all hydrogen atoms were placed in calculated positions and not refined, except for B−H hydrogens which were located in difference maps and refined isotropically. For complex **2**, the material crystallizes with both toluene and hexane in the lattice. In this case, there is a 50:50 mixture of toluene and hexane occupying the same space in the asymmetric unit. Mild restraints were employed to maintain reasonable geometries for both solvent molecules. For complex **4**, the material crystallizes with one disordered molecule of solvent C_5H_{12} in the asymmetric unit. This solvent molecule was modeled in two orientations with isotropic thermal parameters. For complex **5**, the material crystallizes with disordered hexanes in the lattice. This disordered solvent molecule could not be modeled reasonably; therefore, the PLATON/SQUEEZE[46] program was used to correct the data for any unresolved residual electron density in the lattice. The formula and any subsequent values calculated from it reflect the presence of one molecule of hexane in the asymmetric unit. Pertinent bond lengths and angles are presented in Table 2. Full details for **2**−**5** are presented in the Supporting Information.

Acknowledgment. We thank the following for support of this research: University of British Columbia (start-up funds), NSERC (Discovery Grant, Research Tools and Instrumentation Grants, Undergraduate Student Research Awards to Jeffery Bird and Qiming Wu), the Canada Foundation for Innovation (New Opportunities Grant), and the British Columbia Knowledge Development Fund.

Supporting Information Available: Complete crystallographic data for complexes **2**−**5** and NMR spectra for **4**, **5**, **15a**, **15c**, **17a**, and **18a**. This material is available free of charge via the Internet at http://pubs.acs.org.

OM700564T

(42) *Bruker SAINT software package*, version 7.03A; Bruker AXS Inc.: Madison, WI, 1997−2003.

(43) *Bruker SAINT software package*, Version 2.10; Bruker AXS Inc.: Madison, WI, 2003.

(44) Altomare, A.; Burla, M. C.; Camalli, M.; Cascarano, G. L.; Giacovazzo, C.; Guagliardi, A.; Moliterni, A. G. G.; Polidori, G.; Spagna, R. *J. Appl. Cryst.* **1999**, *32*, 115−119.

(45) *Bruker SAINT software package*, Version 5.1; Bruker AXS Inc.; Madision, WI, 1997.

(46) Sluis, P. V. D.; Spek, A. L. *Acta Crystallogr., Sect A* **1990**, *46*, 194−201.